

# Modelling of mercury isotope separation in CP stellar atmospheres: results and problems

A. Sapar, A. Aret, L. Sapar, R. Poolamäe

*Tartu Observatory, Tõravere 61062, Estonia*

---

## Abstract

Formation of anomalous isotope abundances in the atmospheres of chemically peculiar (CP) stars can be explained by light-induced drift (LID). This effect is additional to the radiative acceleration and appears due to systematic asymmetry of radiative flux in partly overlapping isotopic spectral line profiles. LID causes levitation of an isotope with a red-shifted spectral line and sinking of an isotope with a blue-shifted line, generating thus diffusive separation of isotopes. We have studied diffusion of mercury as a typical well-studied isotope-rich heavy metal. Our model computations show that in mercury-rich quiescent atmospheres of CP stars LID causes levitation of the heavier mercury isotopes and sinking of the lighter ones. Precise quantitative modelling of the process of isotope separation demands very high-resolution computations and the high-precision input data, including data on hyperfine and isotopic splitting of spectral lines, adequate line profiles and impact cross-sections. Presence of microturbulence and weak stellar winds can essentially reduce the effect of radiative-driven diffusion.

*Key words:* Stars: atmospheres, Stars: chemically peculiar, Stars: abundances, Diffusion, Line: profiles

---

## 1. Introduction

The problem of specifying the physical processes which cause the observed drastic overabundance of several heavy metals and anomalous abundance ratios of their isotopes in the atmospheres of chemically peculiar (CP) stars, especially of chemically peculiar mercury–manganese (HgMn) stars, has been on agenda already for several decades. At the present time almost nobody doubts, that atomic diffusion is responsible for a large part of the abundance variations observed in CP stars. About 40 years ago Michaud demonstrated in his pioneering papers (Michaud, 1970; Michaud et al., 1976) that for spectral line-rich ions of trace elements the gradient of the radiative pressure, i.e. the upwards directed radiative acceleration, essentially exceeds the downwards directed gravity. This circumstance produces the phenomenon of accumulation of spectral line-rich heavy metals in the stellar atmosphere. Further numerous papers have confirmed the result.

Stellar evolution models with radiative-driven diffusion have been constructed by Michaud and his colleagues for AmFm stars (Richer et al., 2000; Michaud et al., 2005), Population II stars (Richard et al., 2002b,a; VandenBerg et al., 2002) and horizontal branch (HB) stars (Michaud et al., 2007, 2008). HB stars are very closely related to HgMn stars. These models do not include detailed atmospheric modelling and assume chemically homogeneous mixed outer region. Radiative accelerations have been

found using so-called “diffusion approximation” for photon flux (Milne, 1927). This approximation is valid in optically thick medium of stellar interiors where  $\tau \gg 1$ . Evolutionary computations show (see Michaud and Richer, 2008, Fig. 1) the high trend of cumulation of heavy metals in the outer layers of stars. Line-rich metals are swept up throughout the stellar interior by upwards directed radiative push. Radiative acceleration on the extremely line-rich low ionization stage ions of heavy metals can exceed downwards directed gravity up to 3 dex.

Stellar evolution models have been relatively successful at explaining peculiarities of AmFm stars. However, not all abundance anomalies of HgMn and HB stars can be reproduced. Isotopic anomalies observed in HgMn stars also remained unexplained. Michaud and Richer (2008) suggested that additional separation occurs in the atmospheric regions.

Observational evidences of abnormal isotope ratios in CP stellar atmospheres have been cumulated during last decade owing to the high-resolution and high signal-to-noise exposures of the HST and ground-based telescopes with similar capabilities. Although the overall picture of isotope variations is complex (see for review Cowley et al., 2008), there is a general regularity for heavy elements to show overabundance of heavier isotopes and for light elements – overabundance of lighter isotopes. For example, isotopic abundances of mercury range from the terrestrial mixture to the virtually pure  $^{204}\text{Hg}$  while overall overabundance of mercury is 4–5 dex (Dolk et al., 2003). In spite of numerous attempts, strong isotopic anomalies observed

---

*Email address:* [sapar@aai.ee](mailto:sapar@aai.ee) (A. Sapar)

in the atmospheres of chemically peculiar stars have not found acceptable explanation yet. Separation of isotopes requires some additional physical mechanism, because the radiative push is almost the same for all isotopes of the particular element.

A possibility for breakthrough was elucidated by Atutov and Shalagin (1988), who, based on the results of laboratory laser experiments, proposed a new physical mechanism, called light-induced drift (LID), for explaining the isotope separation in the quiescent atmospheres of CP stars.

## 2. Concept of LID and its main formulae

The proposal by Atutov and Shalagin (1988) inspired us (Aret and Sapar, 2002; Sapar et al., 2008a,b) to investigate the possibilities to unveil the enigmatic appearance of isotope anomalies in the CP stellar atmospheres using LID phenomenon. This new mechanism is fully based on the asymmetry of spectral lines. It works effectively if spectral line profiles of a studied element are systematically asymmetrical. This is the case for partly overlapping mutually shifted isotopic lines.

The absorption of the radiative flux, which is asymmetrically distributed in the blue and red wings of a spectral line, generates anisotropy of excitation rate of the atomic particles participating in thermal motion. For example, larger radiative flux in the red wing of a spectral line gives more excited particles among those moving downward in the atmosphere than among those moving upward. Particles in excited states have larger collision cross-sections than particles in the ground or lower excitation states and thus the mobility of particles in the higher excited states is smaller. If particles survive in the excited states until the next collision, then their free paths are shorter than free paths of the unexcited particles. This means that radiative flux asymmetry in the spectral lines triggers a diffusion phenomenon.

The first task was to find the formulae describing this phenomenon. We succeeded to reduce the LID to the equivalent acceleration to be added to the usual radiative acceleration (Aret and Sapar, 2002; Sapar et al., 2008b).

As well known, the usual radiative acceleration due to electron transition from lower level  $l$  to upper level  $u$  of ion  $j$  can be found as

$$a_j^{\text{rad}} = \frac{\pi}{m_j c} \int_0^\infty X_{j,l} \sigma_{ul}^0 V(u_\nu, a) \mathcal{F}_\nu d\nu. \quad (1)$$

Here  $m_j$  is the mass of the light-absorbing ion,  $X_{j,l}$  is state  $l$  population fraction,  $\pi \mathcal{F}_\nu$  is total monochromatic flux and  $\sigma_{ul}^0$  is the absorption cross-section in transition  $l \rightarrow u$ :

$$\sigma_{ul}^0 = \frac{\pi e^2 f_{ul}}{m_e c \Delta\nu_D}, \quad (2)$$

where  $f_{ul}$  is oscillator strength and  $\Delta\nu_D$  is Doppler width of the spectral line. Normalized frequency distribution in

a spectral line is the Voigt function, being the convolution of the Lorentz and Doppler profiles, i.e.

$$V(u_\nu, a) = \frac{a}{\pi^{3/2}} \int_{-\infty}^{\infty} \frac{e^{-y^2}}{(u_\nu - y)^2 + a^2} dy. \quad (3)$$

The argument of the Voigt function is the dimensionless frequency  $u_\nu = \Delta\nu/\Delta\nu_D$ , its parameter  $a = \Gamma_{ul}/(4\pi\Delta\nu_D)$  is the ratio of characteristic widths of Lorentz and Doppler profiles. Integration is carried out over the dimensionless velocity  $y = v/v_T$ , where the thermal velocity  $v_T = \sqrt{2kT/m_j}$ .

LID appears due to difference of collision cross-sections in different quantum states. LID efficiency depends on the difference between collision rates in upper and lower state and also on the probability of particle to stay in the excited state until the next collision.

Based on these conceptual standpoints we have derived the following expression for the equivalent acceleration due to LID in the transition  $l \rightarrow u$  of ion  $j$ :

$$a_j^{\text{LID}} = \varepsilon q \frac{\pi}{m_j c} \int_0^\infty X_{j,l} \sigma_{ul}^0 \frac{\partial V(u_\nu, a)}{\partial u_\nu} \mathcal{F}_\nu d\nu. \quad (4)$$

Coefficient  $q$  is the ratio of the mean momentum of the atomic particles and the photon momentum:

$$q = \frac{m_j v_T c}{2h\nu} = \frac{m_j v_T}{2} : \frac{h\nu}{c}. \quad (5)$$

Due to the large value of  $q \approx 10,000$ , LID can be important even in the case of moderate asymmetry of radiative flux in the spectral line profiles. Under favourable conditions LID may be several orders of magnitude larger than usual radiative acceleration in line. Efficiency of LID  $\varepsilon$  is given by

$$\varepsilon = \frac{C_u - C_l}{C_u} \cdot \frac{C_u}{A_u + C_u} = \frac{C_u - C_l}{A_u + C_u}, \quad (6)$$

where  $A_u$  is the total rate of radiative transitions from the upper state. The first term in Eq.(6) is the relative difference between collision rates in upper and lower states. The second term expresses the probability that during the free flight after photon absorption de-excitation does not happen. Unlike the amplification coefficient  $q$ , the value of  $\varepsilon$  can be estimated only with rather low precision. Characteristic values of  $\varepsilon$  are from about  $10^{-3}$  in the outer atmospheric layers of the CP stars to about 1/4 in the deep layers.

Quantum state life-times have been estimated similarly to the Kurucz spectrum synthesis program SYNTHE (Kurucz, 1993) according to the formulae given in the book by Kurucz et al. (1974). Radiative and Stark damping constants by Proffitt et al. (1999) were used for the lines given in their paper. Cross-sections of mercury collisions with buffer gas (H + He) particles in the upper state  $u$  are larger than in the lower state  $l$ . These collisions are predominantly elastic. The collision cross-sections were calculated

adopting the quasi-hydrogenic approximation. For ion-impacts also the additional Coulomb repulsive cross-sections were taken into account. Diffusion coefficients were calculated according to the Gonzalez et al. (1995). These approximations allow to study general trends of isotope separation due to LID. More detailed computations of cross-sections and quantum state life-times are necessary in the future studies, but general picture should remain the same.

The total effective acceleration, acting on atomic particle due to both the radiative force and the LID is given by  $a_j^t = a_j^{\text{rad}} + a_j^{\text{LID}}$ . Thus, the effect of the light-induced drift can be incorporated by replacing the Voigt function  $V(u_\nu, a)$  in the expression of radiative acceleration Eq.(1) by

$$W(u_\nu, a) = V(u_\nu, a) + \varepsilon q \frac{\partial V(u_\nu, a)}{\partial u_\nu}. \quad (7)$$

Once again, we would like to emphasize, that the LID can be treated as acceleration generated by additional specific force.

Light-induced drift is most effective in the intermediate layers of stellar atmospheres. In high layers of atmosphere or above it LID efficiency is small because of long free paths of the particles, i.e. probability of particle to return to the lower state before the next collision is larger. In stellar interiors LID is inessential compared to the usual radiative acceleration due to other effects: first, isotopic splitting of lines of high ions (e.g. Hg III, IV etc.) is so large that isotopic lines do not overlap and consequently do not give a systematic asymmetry of the lines generating large LID; second, radiative flux becomes local and asymmetry of flux diminishes.

### 3. On the isotopic and hyperfine splitting of spectral lines

The efficiency of the LID phenomenon is governed by the finest details of spectral line splitting, including their hyperfine and isotopic structure, which determines the regularities in the spectral line overlapping and thus the degree of their asymmetry. General expression for energy shift of quantum states of isotope with mass  $M$  is sum of the normal (virial), specific (the momentum correlation of nucleons) and field (nuclear volume) shifts. Symbolically, it can be expressed in the form

$$\Delta E_M = -\frac{m_e}{M} E_0 + E_s + E_A. \quad (8)$$

The first term here is the normal shift, being, as seen from the expression, large for light element isotopes and small for the heavy ones. The specific shift gives essential contribution only for the medium weights atoms with  $Z = 10, \dots, 20$ , and its computation is rather complicated. The third term is the nuclear volume shift due to symmetric charge distribution in the nucleus, depending on the integrated product of the mean charge density in nucleus

and on the square radius of nucleus, i.e. approximately holds

$$E_A \propto \langle \rho_e r_M^2 \rangle,$$

where  $\rho_e$  is charge density in the nucleus and  $r_M$  is current value of the radius. As well known, only the s-state electrons have non-zero charge in the centre of nucleus. Therefore, the volume shift has largest contribution for s-electrons and it is essentially lower for the other states.

If nucleus is a sphere with radius  $R$  and charge distribution is uniform in it, then

$$R^2 = \frac{5}{3} \langle r_M^2 \rangle.$$

For atoms with mass number  $A > 16$  holds approximately (in fm units)  $R = 1.1154A^{1/3}$  and thus

$$E_A \propto \rho_e A^{2/3}. \quad (9)$$

Naturally, this formula gives only a rough approximation for the volume shifts. As seen from the Eq.(9), the volume shift grows monotonously with atomic weight contrary to the normal shift, which diminishes for the heavier nuclei.

In the isotopes with odd number of nucleons presence of magnetic dipole momentum of nucleus and anisotropy of the charge distribution generate the atomic energy level shifts due to total magnetic dipole and electric quadrupole momenta of nucleus, correspondingly. The spectral line shifts of the bound states which appear due to magnetic dipole, are specified by

$$W_{H2} = \frac{A}{2} C \quad (10)$$

and due to quadrupole momentum

$$W_{E4} = B \frac{\frac{3}{4} C(C+1) - I(I+1) - J(J+1)}{2I(2I-1)2J(2J-1)}, \quad (11)$$

where

$$C = F(F+1) - I(I+1) - J(J+1). \quad (12)$$

In these formulae  $I$  and  $J$  are the nuclear and total electron angular momentum quantum numbers, respectively, and  $F$  is their vector sum. The quantities  $A$  and  $B$  depend correspondingly on the magnetic dipole and electric quadrupole momenta of the atomic nucleus.

### 4. Separation of mercury isotopes in CP stellar atmospheres

Generation of elemental and isotopic peculiarities in the atmospheres of CP stars is described by the following scenario. During stellar evolution line-rich heavy metals are pushed to the atmosphere from stellar interiors due to the large expelling radiative force which can exceed the gravity by several dex (Michaud and Richer, 2008). However, this radiative drive leaves solar isotope ratios unaltered.

Isotope separation takes place in stellar atmospheres, where the local diffusive radiative transfer is replaced by non-local radiative transfer. This favours generation of asymmetrical radiative flux in profiles of spectral lines. Flux asymmetry within spectral line profiles of atoms and ions generates light-induced drift, which is not random but cumulative for isotopes, because isotopic splitting of spectral lines creates systematic asymmetry in overlapping line profiles.

Study of evolutionary separation of heavy metals, predominantly of Hg, and their isotopes due to LID in the atmospheres of CP stars has been an essential topic of our investigations during about last decade. Computer code SMART (Sapar and Poolamäe, 2003; Sapar et al., 2007; Aret et al., 2008), composed primarily for modelling of stellar atmospheres and stellar spectra, has been supple-

mented with additional software blocks for computation of evolutionary scenarios of diffusive separation of isotopes of chemical elements due to radiative acceleration, LID and gravity. Mercury has been chosen for the modelling mainly because of two reasons. First, it is a typical isotope-rich heavy metal. Second, mercury is highly overabundant in HgMn stars and its isotopic mixture has been determined from observations for more than 30 stars (Woolf and Lambert, 1999; Dolk et al., 2003).

It has turned out that formation of anomalous isotope abundances in stellar atmospheres, including the dominance of the heaviest isotope, cannot be explained by the diffusion theory without including LID mechanism.

Since LID is sensitive to the shape of spectral lines, synthetic spectra must be computed with high resolution at all layers of model atmosphere. Radiative flux in optically

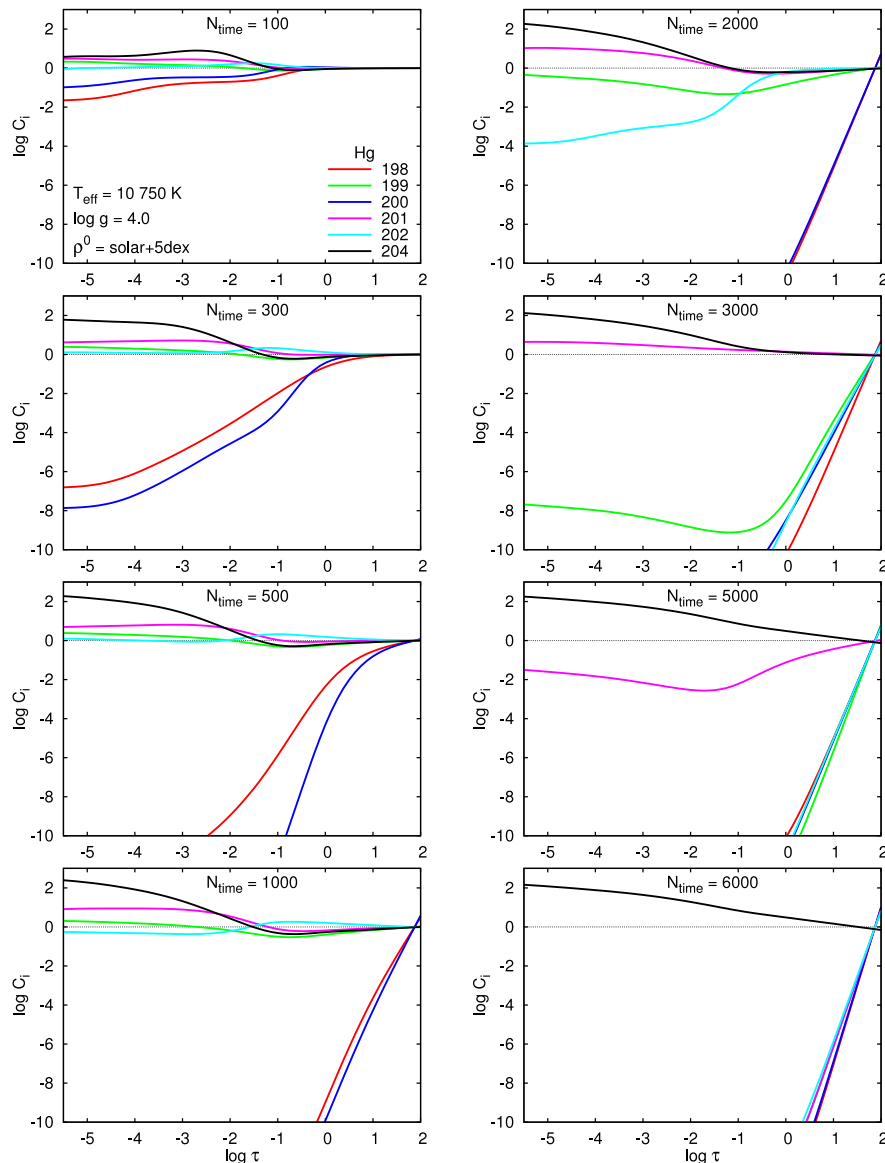


Figure 1: Evolutionary changes of mercury isotope concentrations relative to the initial ones  $C_i = \rho_i / \rho_i^0$  in model atmosphere with  $T_{\text{eff}} = 10\,750\text{ K}$ ,  $\log g = 4$ ,  $V_{\text{rot}} = 0$ ,  $V_{\text{turb}} = 0$  and initial Hg abundance solar + 5 dex with solar system isotope ratios.

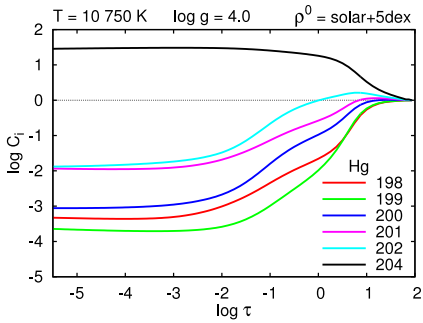


Figure 2: Equilibrium mercury concentrations  $C_i = \rho_i/\rho_i^0$  in model atmosphere with microturbulence. Microturbulent diffusion coefficient is assumed to be 50 times the atomic diffusion coefficient. Model parameters:  $T_{\text{eff}} = 10\,750\text{ K}$ ,  $\log g = 4$ ,  $\rho_i^0 = \text{solar} + 5\text{ dex}$ .

thin medium of stellar atmosphere has to be found resolving the radiative transfer equation in detail. This is more difficult and time-consuming than computing the flux according to the so-called diffusion approximation, valid in optically thick media of stellar interiors. Precise data on hyperfine and isotopic splitting of spectral lines and cross-sections of various physical processes are also necessary in LID computations.

Spectral line data for mercury have been compiled using different sources and improved by adding isotopic splitting to all available Hg lines. Most of the line data have been taken from the lists by Kurucz and Bell (1995) and Vienna atomic line database VALD (Kupka et al., 2000). Hyperfine and isotopic structure of Hg lines and their oscillator strengths available in papers by Proffitt et al. (1999) and Smith (1997) were used to improve our line list. For other lines isotopic splitting was calculated using relative shifts found by Striganov and Dontsov (1955), scaled to units  $[202 - 200] = 1$ , giving for other splitted line components  $[198 - 200] = -0.94$ ,  $[199 - 200] = -0.80$ ,  $[201 - 200] = 0.30$ ,  $[204 - 200] = 1.98$ . For scaling these relative shifts to wavenumbers, we have taken into account that  $[202 - 200] = 0.179\text{ cm}^{-1}$  for Hg I,  $[202 - 200] = 0.508\text{ cm}^{-1}$  for Hg II and  $[202 - 200] = 0.600\text{ cm}^{-1}$  for Hg III. Compiled line list contains about 700 resonance and low excitation spectral lines in the wavelength range approximately 800–12,000 Å for Hg I, Hg II and Hg III, i. e. for ion species, which are most important for LID.

In this paper we present some results of modelling the evolutionary separation of mercury isotopes and discuss some problems on the way of further studies. The problems of LID modelling in the quiescent atmospheres of slowly rotating CP stars involve the computation of line strengths, formation of line profiles due to different microphysical interaction processes, but also formation of microturbulence and weak stellar winds as the phenomena, reducing the diffusion. In addition, presence of entangled magnetic field can affect the formation of anomalous isotope abundances, mainly due to Zeeman splitting of spectral lines.

Example of a computed evolutionary scenario of sep-

aration of mercury isotopes due to LID in mercury-rich (solar + 5 dex) main sequence stellar atmosphere ( $T_{\text{eff}} = 10\,750\text{ K}$ ,  $\log g = 4$ ,  $V_{\text{rot}} = 0$ ,  $V_{\text{turb}} = 0$ ) is given in Fig. 1. Macromotions that can suppress diffusion effects have been ignored. Consequent frames show relative changes of mercury isotopic abundances  $C_i = \rho_i/\rho_i^0$  with time throughout the atmosphere ( $-6 < \log \tau < 2$ ). Lighter even-A isotopes sink first. Odd-A isotopes are supported longer in the atmosphere due to hyperfine splitting of their spectral lines. As stated above, the hyperfine splitting of atomic states is essential only for odd-A isotopes. Hyperfine splitting mixes the order of isotope lines and makes the picture of evolutionary isotope separation more complicated. However, as time passes, all lighter isotopes sink and only the heaviest isotope  $^{204}\text{Hg}$  remains in the atmosphere. Separation in upper layers of the atmosphere proceeds essentially faster than in deep layers. We would like to emphasize that present evolutionary scenario has been computed for perfectly quiet stellar plasma, without microturbulence, stellar wind or any other mixing process. Presence of macromotions in the atmosphere drastically slows down the diffusion and also reduces resulting abundance gradients.

Final equilibrium isotope separation profiles throughout the atmosphere in the presence of microturbulence (Fig. 2) have been iteratively computed for the same model atmosphere as the evolutionary scenario presented in Fig. 1. Microturbulent diffusion coefficient has been assumed to exceed the atomic diffusion coefficient 50 times. The heaviest isotope  $^{204}\text{Hg}$  is also strongly dominant, however abundance gradients are not as steep as in Fig. 1.

Light-induced drift is generated when the radiative flux is asymmetric within the line widths of the light-absorbing ion. This asymmetry mainly appears due to line blendings, which are usually random. Thus, a direction and value of the LID in each spectral line is also random and total LID, obtained summing over all spectral lines of studied element, is minor. Total value of LID can be large only if there is a systematic asymmetry of spectral lines, what is the case for the overlapping isotopic lines. Thereby LID of

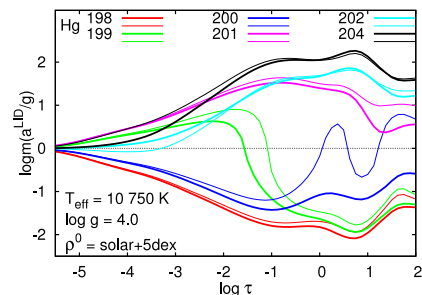


Figure 3: Effect of line blendings on LID of Hg isotopes. Accelerations of the Hg isotopes due to LID at the first time step (i.e. with homogeneous Hg abundance) are shown in the modified logarithmic scale  $\log m\left(\frac{a}{g}\right) = \text{sign}(a) \log\left(\left|\frac{a}{g}\right| + 1\right)$ . Thick lines: only Hg isotopic lines, no blendings with lines of other elements; thin lines: lines of all elements are present.

mercury isotopes is governed by mutual overlaps of their spectral lines, while blendings with lines of other elements are less important, because they statistically cancel out. Calculations of LID due to overlapping lines of mercury isotopes in the presence and without lines of other elements confirm this conclusion (Fig. 3). Blendings with lines of other elements certainly affect values of  $a^{\text{LID}}$ , but do not change the main regularities defined by mutual overlaps of Hg isotopic lines.

## 5. Hydrogenic line profiles

Although details of mercury lines are crucial for computation of LID acceleration, also profiles of all strong lines, which overlap with mercury lines, should be computed with high precision to obtain more realistic picture of isotope separation. This concerns also the hydrogen spectral line series. As we have shown (Sapar et al., 2006), the convolution of Holtsmark, Lorentz and Doppler profiles in the result of two analytical integrations reduces to the sum of three contribution terms, namely

$$\Phi(\beta) = \chi(\beta) + \Lambda(\beta) + \Delta(\beta), \quad (13)$$

where

$$\chi(\beta) = \frac{2}{\pi} \int_0^\infty \beta x \sin(\beta x) \varepsilon(x) dx, \quad (14)$$

$$\Lambda(\beta) = \frac{2L}{\pi} \int_0^\infty x \cos(\beta x) \varepsilon(x) dx, \quad (15)$$

$$\Delta(\beta) = \frac{4D^2}{\pi} \int_0^\infty x^2 \cos(\beta x) \varepsilon(x) dx \quad (16)$$

and

$$\varepsilon(x) = \exp\left(-x^{3/2} - Lx - D^2x^2\right). \quad (17)$$

In these formulae  $\beta = (\nu - \nu_0)/\Delta\nu_S$ ,  $L = \Delta\nu_L/\Delta\nu_S$  and  $D = \Delta\nu_D/2\Delta\nu_S$ . Here  $\Delta\nu_D$ ,  $\Delta\nu_L$  and  $\Delta\nu_S$  are the widths parameters of Doppler, Lorentz and Holtsmark line profiles, respectively.

Another possibility is numerical integration of the convolution of analytical high-precision approximation expressions of Holtsmark and Voigt functions (Sapar et al., 2006). The asymptotic series expansions for the small and large values of argument  $\beta$  have been found by us as a contribution to this approach. For the intermediate region the exponential term can be expanded into series followed by integration over circle.

For main sequence stars Holtsmark distribution shielded by the Debye radius, i.e. the Ecker correction is not essential, because the value of screening parameter, approximately estimated by

$$\delta = \frac{4\pi R_D^3}{3} N, \quad (18)$$

where  $R_D$  is the Debye radius

$$R_D = \left(\frac{kT}{4\pi e^2 N}\right)^{1/2} \quad (19)$$

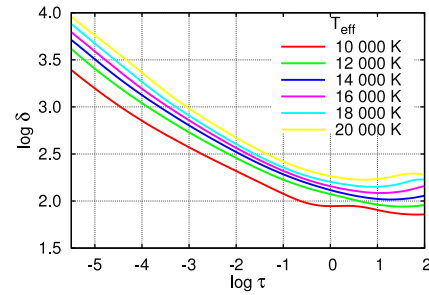


Figure 4: Number of charged particles in the Debye sphere. Large Ecker coefficient values  $\delta > 50$  show that Holtsmark distribution is valid throughout stellar atmospheres.

and  $N$  is the number density of charged particles, has large values up to deep atmospheric layers. This is illustrated in Fig. 4. As known, Holtsmark distribution holds well if  $\delta$ , being the number of particles inside the Debye sphere, exceeds about 50.

As mentioned earlier, an important problem for modelling of stellar atmospheres is to find high-precision profile function for hydrogen lines. The Model Microfield Method (MMM) initially developed by Frisch and Brissaud (1971) and Brissaud and Frisch (1971) and further elaborated by Stehlé et al. (e.g. Stehlé, 1990; Stehlé and Jacquemot, 1993) takes statistically into account also the ion dynamics effects. Tables for the Lyman and Balmer (Stehlé, 1994; Stehlé and Hutcheon, 1999), Paschen (Stehlé, 1996) and Brackett lines (Stehlé and Fouquet, 2009) have been calculated and are available for astrophysical applications. The main difference between MMM and Holtsmark profiles lies in the line centre. The profile function obtained with MMM has a non-zero plateau at small argument values while the Holtsmark distribution approaches zero. However, the total contribution of blendings with hydrogen lines to the LID of mercury isotopes turned out to be minor and eventually also the MMM correction does not essentially affect our results.

Splitting of H spectral lines due to the linear Stark effect, where the number of splitted line components grows rapidly towards the higher members of the series, also must be further taken into account. This problem is connected with determination of dissolution rates of high Rydberg lines. The state survival fractions have been specified at least in three different ways, giving the expressions in the form

$$W_n = CN^k n^m, \quad (20)$$

where  $N$  is the number density of charged particles and  $n$  is the current value of the principal quantum number. These methods are:

- Inglis–Teller overlap cutoff ( $W_n = C_1 N^{-1} n^{-7.5}$ ),
- the nearest neighbour dissolution ( $W_n = C_2 N^{-1} n^{-6}$ ) or exponential cutoff, and
- the red-wing Stark components dissolution ( $W_n = C_3 N^{-2/3} n^{-4}$ ).

Different partition functions and their dependence on  $N$  correspond to these cutoff methods.

We have used the last expression not only for H line series, but for smooth transition from Rydberg line series to corresponding continua of all elements. Thus we obtain smooth transition from line series to the corresponding continua, but the state survival fractions are probably somewhat overestimated. It is extremely difficult to describe the real situation, because also a complicated picture of Stark splitting of spectral lines must be taken into account. Although these problems are weakly connected with the LID computations, they are important for modelling of stellar atmospheres and spectra.

## 6. Concluding remarks

Light-induced drift enables to explain and to model evolutionary generation of drastic isotopic anomalies in quiescent CP stellar atmospheres, i.e. if stellar wind, meridional circulation and macroturbulence are lacking. However, microturbulence, which is always present in the atmospheres, diminishes essentially the equilibrium gradients of isotope ratios. Nevertheless, it has been succeeded to explain the main regularity – formation of essentially higher abundances of the heavier isotopes of heavy metals on the example of mercury.

Further refinements of a number of physical process characteristics are needed. The line profile functions and shifts, state survival fractions, impact cross-sections, Stark and hyperfine splitting of spectral lines and several other quantities should be improved to model evolutionary scenarios of isotope separation in CP stellar atmospheres.

## Acknowledgements

We are grateful to a referee for pointing on the necessity of discussion concerning the possible influence of the MMM approach on our model computations. We gratefully acknowledge the financial support by the Estonian Science Foundation grant ETF7691.

## References

Aret, A., Sapar, A., 2002. Light-induced drift for Hg isotopes in chemically peculiar stars. *Astronomische Nachrichten* 323, 21–30.

Aret, A., Sapar, A., Poolamäe, R., Sapar, L., 2008. SMART – a computer program for modelling stellar atmospheres. In: Deng, L., Chan, K.-L. (Eds.), *The Art of Modeling Stars in the 21st Century*. Vol. 252 of IAU Symposium. Cambridge University Press, pp. 41–42.

Atutov, S. N., Shalagin, A. M., 1988. Prospects for light-induced drift in astrophysical objects. *Soviet Astronomy Letters* 14, 284–287.

Brissaud, A., Frisch, U., 1971. Theory of Stark broadening - II. Exact line profile with model microfield. *Journal of Quantitative Spectroscopy and Radiative Transfer* 11, 1767–1783.

Cowley, C. R., Hubrig, S., Castelli, F., 2008. Isotopic anomalies in CP stars: helium, mercury, platinum, and calcium. *Contributions of the Astronomical Observatory Skalnaté Pleso* 38, 291–300.

Dolk, L., Wahlgren, G. M., Hubrig, S., 2003. On the elemental abundance and isotopic mixture of mercury in HgMn stars. *A&A* 402, 299–313.

Frisch, U., Brissaud, A., 1971. Theory of Stark broadening - I. Soluble scalar model as a test. *Journal of Quantitative Spectroscopy and Radiative Transfer* 11, 1753–1766.

Gonzalez, J.-F., LeBlanc, F., Artru, M.-C., Michaud, G., 1995. Improvements on radiative acceleration calculations in stellar envelopes. *A&A* 297, 223–236.

Kupka, F. G., Ryabchikova, T. A., Piskunov, N. E., Stempels, H. C., Weiss, W. W., 2000. VALD-2 – the new Vienna Atomic Line Database. *Baltic Astronomy* 9, 590–594.

Kurucz, R., 1993. SYNTHES spectrum synthesis programs and line data. Kurucz CD-ROM No. 18. Cambridge, Mass.: Smithsonian Astrophysical Observatory.

Kurucz, R., Bell, B., 1995. Atomic line data. Kurucz CD-ROM No. 23. Cambridge, Mass.: Smithsonian Astrophysical Observatory.

Kurucz, R. L., Peytremann, E., Avrett, E. H., 1974. Blanketed model atmospheres for early-type stars. Washington : Smithsonian Institution, Astrophysical Observatory : for sale by the Supt. of Docs., U.S. Govt. Print. Off.

Michaud, G., 1970. Diffusion processes in peculiar A stars. *ApJ* 160, 641–658.

Michaud, G., Charland, Y., Vauclair, S., Vauclair, G., 1976. Diffusion in main-sequence stars - radiation forces, time scales, anomalies. *ApJ* 210, 447–465.

Michaud, G., Richer, J., 2008. Horizontal branch stars as AmFm/HgMn stars. *Contributions of the Astronomical Observatory Skalnaté Pleso* 38, 103–112.

Michaud, G., Richer, J., Richard, O., 2005. Atomic diffusion and  $\alpha$  Leonis. *ApJ* 623, 442–446.

Michaud, G., Richer, J., Richard, O., 2007. Horizontal branch evolution and atomic diffusion. *ApJ* 670, 1178–1187.

Michaud, G., Richer, J., Richard, O., 2008. Abundance anomalies in horizontal branch stars and atomic diffusion. *ApJ* 675, 1223–1232.

Milne, E. A., 1927. Selective radiation-pressure and the structure of a stellar atmosphere. *MNRAS* 87, 697–708.

Proffitt, C. R., Brage, T., Leckrone, D. S., Wahlgren, G. M., Brandt, J. C., Sansonetti, C. J., Reader, J., Johansson, S. G., 1999. Mercury in the HgMn Stars  $\chi$  Lupi and HR 7775. *ApJ* 512, 942–960.

Richard, O., Michaud, G., Richer, J., 2002a. Models of metal-poor stars with gravitational settling and radiative accelerations. III. Metallicity dependence. *ApJ* 580, 1100–1117.

Richard, O., Michaud, G., Richer, J., Turcotte, S., Turck-Chièze, S., VandenBerg, D. A., 2002b. Models of metal-poor stars with gravitational settling and radiative accelerations. I. Evolution and abundance anomalies. *ApJ* 568, 979–997.

Richer, J., Michaud, G., Turcotte, S., 2000. The evolution of AmFm stars, abundance anomalies, and turbulent transport. *ApJ* 529, 338–356.

Sapar, A., Aret, A., Poolamäe, R., Sapar, L., 2008a. Segregation of isotopes of heavy metals due to light-induced drift: results and problems. *Contributions of the Astronomical Observatory Skalnaté Pleso* 38, 273–278.

Sapar, A., Aret, A., Sapar, L., Poolamäe, R., 2008b. Formulae for study of light-induced drift diffusion in CP star atmospheres. *Contributions of the Astronomical Observatory Skalnaté Pleso* 38, 445–446.

Sapar, A., Poolamäe, R., 2003. “SMART”: a compact and handy FORTRAN code for the physics of stellar atmospheres. In: Hubeny, I., Mihalas, D., Werner, K. (Eds.), *Stellar Atmosphere Modeling*. Vol. 288 of *Astronomical Society of the Pacific Conference Series*. pp. 95–98.

Sapar, A., Poolamäe, R., Sapar, L., 2006. High-precision approximation expressions for line profiles of hydrogenic particles. *Baltic Astronomy* 15, 435–447.

Sapar, A., Poolamäe, R., Sapar, L., Aret, A., 2007. Computation of model atmospheres and spectra of hot stars by programme SMART: results and problems. In: Mashonkina, L., Sachkov, M. (Eds.), *Spectroscopic Methods in Modern Astrophysics*. Janus-K,

- Moscow, pp. 236–254, in Russian.
- Smith, K. C., 1997. Elemental abundances in normal late-B and HgMn stars from co-added IUE spectra V. Mercury. *A&A* 319, 928–947.
- Stehlé, C., 1990. What is meant by low or high densities in the Stark broadening of hydrogenic ion lines? *Journal of Quantitative Spectroscopy and Radiative Transfer* 44, 135–142.
- Stehlé, C., 1994. Stark broadening of hydrogen Lyman and Balmer in the conditions of stellar envelopes. *A&AS* 104, 509–527.
- Stehlé, C., 1996. Paschen lines of hydrogen and  $\text{He}^+$  ion. *Physica Scripta T* 65, 183–187.
- Stehlé, C., Fouquet, S., 2009. Hydrogen Stark broadened Brackett lines. E-print arXiv:0907.0635.
- Stehlé, C., Hutcheon, R., 1999. Extensive tabulations of Stark broadened hydrogen line profiles. *A&AS* 140, 93–97.
- Stehlé, C., Jacquemot, S., 1993. Line shapes in hydrogen opacities. *A&A* 271, 348–359.
- Striganov, A. R., Dontsov, Y. P., 1955. Isotopic effect in atomic spectra. *Uspekhi Fizicheskikh Nauk* 55, 315–390, in Russian.
- VandenBerg, D. A., Richard, O., Michaud, G., Richer, J., 2002. Models of metal-poor stars with gravitational settling and radiative accelerations. II. The age of the oldest stars. *ApJ* 571, 487–500.
- Woolf, V. M., Lambert, D. L., 1999. Mercury elemental and isotopic abundances in mercury-manganese stars. *ApJ* 521, 414–431.